Two-dimensional solitary waves in media with quadratic and cubic nonlinearity

Ole Bang

Australian Photonics Cooperative Research Center, Research School of Physical Sciences and Engineering, Optical Sciences Centre, Australian National University, Canberra ACT 0200, Australia

We numerically determine the existence and stability regimes of bright 2+1 dimensional spatial solitary waves (solitons) in media with quadratic and focusing cubic nonlinearities. The quadratic nonlinearity enables stable solitons to exist when the effective cubic nonlinearity is sufficiently weak. We study the dynamics of the solitons in the unstable regime, and demonstrate the existence of two different nonlinear Schrödinger limits.

I. INTRODUCTION

The basic theory of cascading and two-wave parametric solitons in materials with a pure quadratic (or $\chi^{(2)}$) nonlinearity is now well understood, and importantly, many of the theoretical results have been confirmed experimentally (see [1] for a recent review). In particular, in bulk media as we consider here, families of stable spatial solitons exist above a certain threshold power [2]. Their excitation from input Gaussian beams has been confirmed experimentally [3], and numerically without walk-off [4], and later with walk-off [5]. In fact it has been shown that self-focusing, leading to a catastrophic collapse, cannot occur in $\chi^{(2)}$ media in any physical dimension [6].

Attention has recently turned to the effect of cubic (or $\chi^{(3)}$) nonlinearity on the known characteristics of solitons and switching in $\chi^{(2)}$ media. The competition between the two types of nonlinearity can, e.g., drastically modify the threshold power for switching [7] and the existence and stability regions of spatial solitary waves diffracting in one transverse dimension (1D) [8–10], and 2D [6,11–13]. It has been shown that the simple model, with only cubic self- and cross-phase modulation (SPM and XPM) terms added to the known equations for $\chi^{(2)}$ media, does not apply to temporal solitary waves, unless the $\chi^{(2)}$ nonlinearity is much weaker than the $\chi^{(3)}$ nonlinearity [10]. Thus, in contrast to $\chi^{(2)}$ media, spatial and temporal solitary waves do not obey the same dynamical equations in media with competing $\chi^{(2)}$ and $\chi^{(3)}$ nonlinearities. The dependence of the threshold power for collapse on the SPM and XPM coefficients have been investigated [6,12], but in the solion studies the cubic nonlinearity has so far been assumed to be dispersionless and the ratio of SPM and XPM terms have been fixed. The effect of different SPM to XPM ratios have only recently been investigated [13].

All $\chi^{(2)}$ materials have an *inherent cubic nonlinearity* that becomes important at high powers or when the fundamental wave (FW) and its second-harmonic (SH) are not perfectly phase-matched. However, this is not the only origin of cubic nonlinearity. When the $\chi^{(2)}$ nonlinearity is periodically varying along the direction of propagation, as in quasi-phase-matched (QPM) media, the effective averaged dynamical equations also include *induced cubic nonlinearities* [14], as a result of incoherent coupling between the wave at the main spatial (QPM) frequency with higher-order modes.

Since competing quadratic and cubic nonlinearities is a general physical phenomenon, it is important to know the effect of such a competition. In this work we present a complete map of the dynamic properties and existence and stability regimes of the three classes of 2D spatial solitary waves existing in $\chi^{(2)}$ media when inherent focusing and dispersionless cubic nonlinearity is taken into account. The defocusing case was recently considered in [11], whereas the power threshold for collapse in the focusing case was investigated in [6,12].

The paper is organized as follows: In Section II we present the dynamical model and compare it with the models used in earlier works on competing nonlinearities. We then consider the case of a bulk medium with focusing dispersionless $\chi^{(3)}$ nonlinearity, and show in Section III when the different classes of localized stationary solutions exist, and how their profiles look like. In Section IV we discuss the stability of localized stationary solutions. The power threshold for instability is compared with the analytical predictions of virial theory, which is briefly recapitulated in Appendix A. In Section V we look at the specific dynamics "deep" in the collapse unstable regime. Finally, Section VI presents a summary.

II. THE MODEL

We consider beam propagation in lossless bulk $\chi^{(2)}$ media under conditions for type I SHG, when cubic material nonlinearity is taken into account. The dynamics is described by the dimensionless equations [10]

$$i\frac{\partial w}{\partial z} + \nabla_\perp^2 w + w^* v + s(|w|^2 + \rho|v|^2)w = 0, \tag{1}$$

$$2i\frac{\partial v}{\partial z} + \nabla_\perp^2 v - \beta v + \frac{1}{2}w^2 + s(\eta|v|^2 + \rho|w|^2)v = 0, \tag{2}$$

which are valid when spatial walk-off is negligible, and both the fundamental frequency, ω_1, and its second har-

monic, $\omega_2{=}2\omega_1$, are far from resonances. The slowly varying complex envelope function of the FW, $w{=}w(\vec{r},z)$, and its SH, $v{=}v(\vec{r},z)$, are assumed to propagate with a constant polarization, $\vec{e}_1$ and $\vec{e}_2$, along the z-axis. The transverse Laplacian $\nabla_\perp^2$ refers to the spatial coordinates $\vec{r}{=}(x,y)$. The electric field $\vec{E}{=}\vec{E}(\vec{R},Z,T)$ is given by

$$\vec{E} = E_0[w\mathrm{e}^{i\theta_1}\hat{e}_1 + 2v\mathrm{e}^{i2\theta_1}\hat{e}_2] + \mathrm{c.c.}, \tag{3}$$

in physical coordinates, where $\vec{R}{=}r_0\vec{r}$, $Z{=}z_0 z$, and $\theta_1{=}k_1 Z-\omega_1 T$. The real normalization parameters E_0, z_0, and r_0, are given by (for details see [10])

$$E_0 = \frac{4\tilde{\chi}_1^{(2)}}{3|\tilde{\chi}_{1s}^{(3)}|},\ z_0 = 2k_1 r_0^2,\ r_0^2 = \frac{3|\tilde{\chi}_{1s}^{(3)}|}{16\mu_0\omega_1^2(\tilde{\chi}_1^{(2)})^2}, \tag{4}$$

where μ_0 is the vacuum permeability and k_n the wavenumber at the frequency ω_n. The real parameters β, s, η, and ρ are given by [10]

$$\beta = 2z_0\Delta k,\ s = \mathrm{sign}(\tilde{\chi}_{1s}^{(3)}),\ \eta = \frac{16\tilde{\chi}_{2s}^{(3)}}{\tilde{\chi}_{1s}^{(3)}},\ \rho = \frac{8\tilde{\chi}_{1c}^{(3)}}{\tilde{\chi}_{1s}^{(3)}}, \tag{5}$$

where $\Delta k{=}2k_1{-}k_2{\ll}k_1$ is the phase-mismatch parameter, and $\tilde{\chi}_n^{(j)}{=}\tilde{\chi}^{(j)}(\omega_n)$ denote the Fourier components at frequency ω_n of the jth order susceptibility tensor. Thus $\tilde{\chi}_1^{(2)}{=}\tilde{\chi}_2^{(2)}$ represents the quadratic nonlinearity, and $\tilde{\chi}_{ns}^{(3)}$ and $\tilde{\chi}_{1c}^{(3)}{=}\tilde{\chi}_{2c}^{(3)}$ the parts of the cubic nonlinearity responsible for SPM and XPM, respectively. Compared with standard notation these coefficients refer to $\tilde{\chi}_{ns}^{(3)}{=}\tilde{\chi}^{(3)}(\omega_n{=}\omega_n-\omega_n+\omega_n)$ and $\tilde{\chi}_{nc}^{(3)}{=}\tilde{\chi}^{(3)}(\omega_n{=}\omega_n-\omega_{3-n}+\omega_{3-n})$.

In the form they appear in here, Eqs (1-2) were used to study collapse in media with an arbitrary number of transverse dimensions [6], and to study bright 2D solitons in the defocusing ($s{=}{-}1$) [11] and focusing case ($s{=}{+}1$) [12,13]. After a simple transformation they correspond to the 1D equations earlier used in [8,9], and later derived rigorously in [10]. Similar equations were recently shown to describe the dynamics in QPM $\chi^{(2)}$ media [14].

The system (1-2) conserves the Hamiltonian H,

$$H = \int [|\nabla_\perp w|^2 + |\nabla_\perp v|^2 + \beta|v|^2 - \mathrm{Re}(w^2 v^*) - \frac{s}{2}(|w|^4 + \eta|v|^4 + 2\rho|wv|^2)]\, d\vec{r}, \tag{6}$$

and the dimensionless power P,

$$P = \int (|w|^2 + 4|v|^2)\, d\vec{r} = P_w(z) + 4P_v(z), \tag{7}$$

which corresponds to the physical power $P_0 P$, where the normalization parameter $P_0{=}0.5\sqrt{\epsilon_0/\mu_0}E_0^2 r_0^2$ is inverse proportional to $\tilde{\chi}_{1s}^{(3)}$ and independent of $\chi^{(2)}$. Furthermore, Eqs. (1-2) are invariant to the phase rotation

$$w \to w\,\mathrm{e}^{i\alpha_0},\quad v \to v\,\mathrm{e}^{i2\alpha_0}, \tag{8}$$

and the Galilean transformation

$$\begin{aligned} w(x,z) &\to w(x-2\alpha_1 z, z)\,\mathrm{e}^{i\alpha_1(x-\alpha_1 z)}, \\ v(x,z) &\to v(x-2\alpha_1 z, z)\,\mathrm{e}^{i2\alpha_1(x-\alpha_1 z)}, \end{aligned} \tag{9}$$

where $\alpha_{0,1}$ are real constants.

Without knowing the experimental setting, and thus the specific values of the $\chi^{(2)}$ and $\chi^{(3)}$ susceptibilities, it is difficult to estimate the values of the dimensionless coefficients η and ρ. However, for a large class of materials and experimental settings, we can neglect the dispersion of $\chi^{(3)}$ and set $\tilde{\chi}_{1s}^{(3)}{=}\tilde{\chi}_{2s}^{(3)}$, and it is further reasonable to set $\tilde{\chi}_{1s}^{(3)}{=}\tilde{\chi}_{1c}^{(3)}$. In this case we get $\eta{=}2\rho{=}16$, which we use below. These values were also used in earlier works on competing $\chi^{(2)}$ and $\chi^{(3)}$ nonlinearities [8–12]. Furthermore, in this papers we consider only the case of focusing cubic nonlinearity, and thus $s{=}{+}1$. For the defocusing case, the existence, stability, and generation of bright solitary waves was analyzed in Ref. [11].

III. LOCALIZED STATIONARY SOLUTIONS

We consider exponentially localized bright solitary wave solutions (with no nodes, i.e., lowest order bound states) of the form

$$w(\vec{r},z) = w_0(r)\mathrm{e}^{i\lambda z},\ v(\vec{r},z) = v_0(r)\mathrm{e}^{i2\lambda z}, \tag{10}$$

where the real functions w_0 and v_0 decay monotonically to zero as $r{=}\sqrt{x^2+y^2}$ increases. Inserting this solution into Eqs. (1-2), we obtain the stationary equations

$$\begin{aligned} &\nabla_\perp^2 w_0 - \lambda w_0 + w_0 v_0 + s(w_0^2 + \rho v_0^2)w_0 = 0, \\ &\nabla_\perp^2 v_0 - (\beta + 4\lambda)v_0 + \frac{1}{2}w_0^2 + s(\eta v_0^2 + \rho w_0^2)v_0 = 0. \end{aligned} \tag{11}$$

There are three main types of localized stationary solutions to Eqs. (11) of the form (10): The Combined or C-solution, where both components are nonzero, $w_0{>}0$ and $v_0{>}0$, and have no particular relative size. This solution can generally only be found numerically, even in 1D [8,10].

It is well-known that when the effective mismatch is large the cascaded nonlinearity has effective cubic properties. In this limit, where $\beta{\gg}1$ and $\beta{\gg}\lambda$, the C-solutions asymptotically develop into the single w-component or W-solution, for which the SH is weak and slaved to the FW, $v_0{\approx}w_0^2/(2\beta)$. The FW is the solution to the 2D nonlinear Schrödinger (NLS) equation

$$\nabla_\perp^2 w_0 - \lambda w_0 + w_0^3 = 0, \tag{12}$$

with power $\mathcal{P}_W{\simeq}P_w{=}P_{\mathrm{nls}}^{\mathrm{c}}$. Here $P_{\mathrm{nls}}^{\mathrm{c}}{=}11.69$ is the threshold power for collapse of solutions to the 2D NLS equation (12) [16]. An analytical expression for the solution

is not known, but a good approximation can be found by the variational technique to be [17]

$$w_0(r) = A_0\sqrt{\lambda}\,\mathrm{sech}(B_0\sqrt{\lambda}\,r) \tag{13}$$

where A_0^2=12ln2/(4ln2-1) and B_0^2=6ln2/(2ln2+1).

In order for C- and W-solutions (with $w_0>0$ and $v_0>0$) to be exponentially localized (i.e. have a purely exponential decay in the tails $r\to\infty$), the real propagation constant λ must be above cut-off $\lambda>\lambda_{\rm cut}\equiv\max\{0,-\beta/4\}$.

The single v-component or V-solution exists for $\eta>0$. It has no FW, $w_0=0$, and its SH is the solution to the 2D NLS equation

$$\nabla_\perp^2 v_0 - (\beta+4\lambda)v_0 + \eta v_0^3 = 0, \tag{14}$$

with power $\mathcal{P}_V=4P_v=4P_{\rm nls}^{\rm c}/\eta$, approximately given by

$$v_0(r) = A_0\sqrt{(\beta+4\lambda)/\eta}\,\mathrm{sech}(B_0\sqrt{\beta+4\lambda}\,r), \tag{15}$$

Since $w_0=0$ the cut-off for the V-solution is different from that of the C-solution, i.e. $\lambda>-\beta/4$.

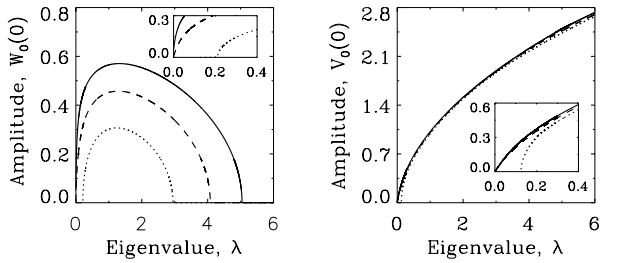

FIG. 1. Amplitude versus λ of (left) the FW and (right) the SH, for the C-solutions with β=−0.5 (dotted), β=0 (dashed), and β=0.5 (solid). $\eta=2\rho=16$, $s=+1$.

Using a standard relaxation technique, we have numerically found the families of C- and V-solutions for $\lambda>\lambda_{\rm cut}$ In Fig. 1 we show the amplitudes $w_0(0)$ and $v_0(0)$ of the C-solution as function of λ for β=0,±0.5. We see that the C-solutions exist only in a certain region, $\lambda_0\le\lambda\le\lambda_1$, which increases with β. For positive β the lower limit is zero, λ_0=0, while for negative β it is close to, but larger than, the cut-off $\lambda_{\rm cut}$ (see inserts in Fig. 1 and Fig. 4) and increases with decreasing β. The upper limit λ_1 always increases with β. Thus no C-solutions will exist for β less than a critical value $\beta_{\rm cr}$, which we find to be $\beta_{\rm cr}$=−0.914. The V-solutions exist for all values of β and $\lambda>\lambda_{\rm cut}$, and its amplitude is close to the prediction given by Eq. (15). At $\lambda=\lambda_1$ the C-solution bifurcates into the V-solution. For negative β this also occurs at λ_0.

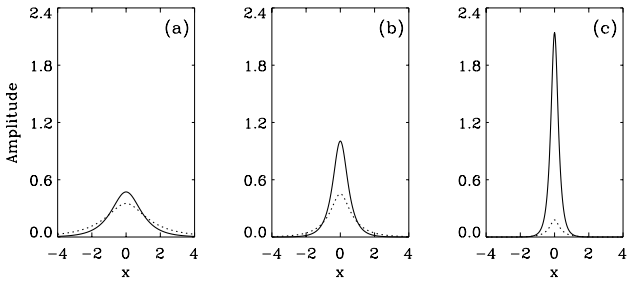

FIG. 2. Profiles $w_0(r=x)$ (dotted) and $v_0(r=x)$ (solid) of the C-solutions shown in Fig. 1 for β=0 and (a) λ=0.3, (b) λ=1, and (c) λ=3.8.

The profiles of the C-solutions are shown in Fig. 2 for β=0, and three representative values of λ, being in the center of the existence region, and close to the edges $\lambda_0=\lambda_{\rm cut}$=0 and λ_1=4.04, respectively. We clearly see that the C-solution gradually becomes narrower and approaches the V-solution with w_0=0, as λ increases towards λ_1. Also, as expected, the profile becomes more and more delocalized as the cut-off $\lambda_{\rm cut}$ is approached.

¿From Fig. 3 with λ=1 and β=4, 10, and 20, we see how the C-solution asymptotically develops into the W-solution with the SH not just being much weaker, but also much narrower, than the FW. In contrast as the V-solution is approached, the FW and SH seem to have approximately the same width (see Fig. 2c).

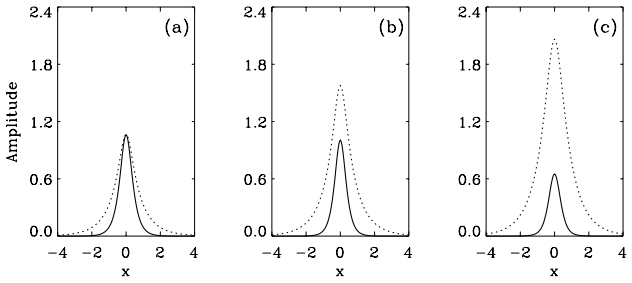

FIG. 3. Profiles $w_0(r=x)$ (dotted) and $v_0(r=x)$ (solid) of the C-solutions shown in Fig. 1 for λ=1 and (a) β=4, (b) β=10 and (c) β=20.

We have made a series of calculations as shown in Fig. 1, and identified the regions of existence of the different types of localized solutions (10) to Eqs. (11) in the parameter plane (λ,β). The results are summarized in Fig. 4, where we have defined the W-solutions as the C-solutions in which more than 90% of the power is concentrated in the FW.

We see that the C-solutions exist above cut-off, $\lambda>\lambda_{\rm cut}$, when $\beta>\beta_{\rm cr}=-0.914$, while the V-solutions always exists above cut-off. As expected, the C-solutions develop into the W-solutions for $\beta\gg\lambda$. However, it is not necessary that $\beta\gg1$ as assumed in obtaining the W-solution (13).

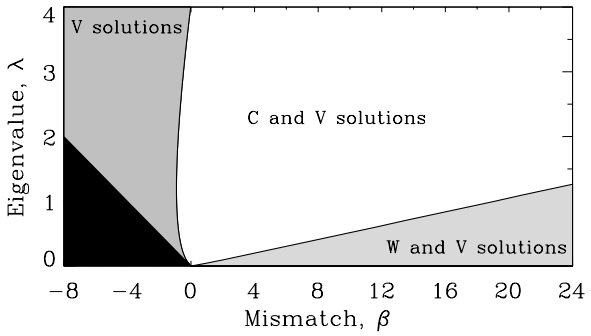

FIG. 4. Regions of existence of C, V, and W-solutions in the (λ, β)-plane. The W-solutions are defined as when 90% of the total power P is in the FW. In the black region $\lambda \leq \lambda_{\rm cut}$ and no localized solutions exists. η=2ρ=16, s=+1.

IV. STABILITY OF SOLITARY WAVES

In Section III we showed that at least two types of localized stationary solutions of the form (10) can co-exist for given values of the mismatch β and power P: The C- and V-solutions. Further numerical analysis shows that in general these two solutions do not exist with equal values of the power P, and when they do, the Hamiltonian of the V-solution is always larger than that of the C-solution. An example of this is shown in Fig. 5 for β=0.

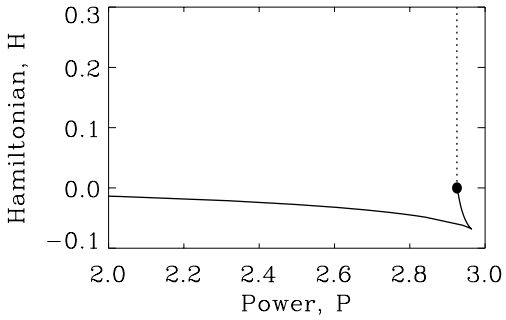

FIG. 5. Hamiltonian H versus total power P for the C-solutions (solid) and V-solutions (dotted), at β=0. The two bifurcate into each other at the point marked with a filled circle, corresponding to λ=λ_1 (see Fig. 1). η=2ρ=16, s=1.

Consequently, when the two solutions coexist, the V-solution is always unstable and the C-solution correspond to the ground-state solutions, whose stability properties we will determine in this section using the Vakhitov-Kolokolov (VK) criterion, requiring positive (negative) $dP/d\lambda$ for stability (instability) [15]. It is well-known that the VK criterion applies to equations of the NLS type [18]. In the case of pure $\chi^{(2)}$ nonlinearity, it has been argued that the VK criterion also apply to solitons supported by two-wave (or type I) SHG [19], and three-wave (or type II) SHG [20], using an adiabatic perturbation technique, and later for Type II SHG [21] using spectral operator theory, as originally by Vakhitov and Kolokolov. Her we will simply use the theorem and test it numerically. A mathematical proof of its validity is in progress.

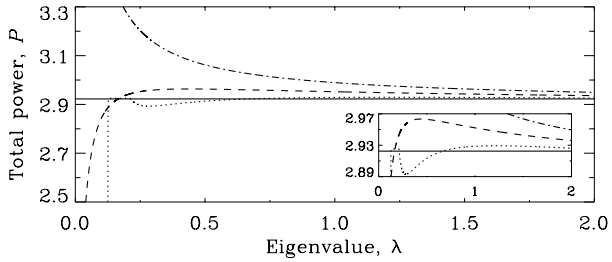

FIG. 6. Power P versus λ for the solutions shown in Fig. 1, with β=−0.5 (dotted), β=0 (dashed), and β=0.5 (dash-dotted). The solid line indicates the value $\mathcal{P}_V$=2.92 and the vertical dotted line indicates $\lambda_{\rm cut}$=−1/8.

In Fig. 6 we show the soliton power P versus λ for three values of β. The power of the V-solution, $\mathcal{P}_V$, is approached as λ increases towards the bifurcation point λ_1. Furthermore, for β=−0.5, the solution is also the V-solution for $\lambda_{\rm cut}$<λ≤λ_0, and therefore the power is also $\mathcal{P}_V$. According to the VK criterion, the solitons are unstable in the whole region of their existence for β=0.5, whereas a critical value of λ exists at phase-matching, β=0, which separate stable and unstable regions. As the mismatch is further decreased to $\beta = -0.5$, the soliton family exhibits a more complex multistable behavior, the derivative $dP/d\lambda$ changing sign several times.

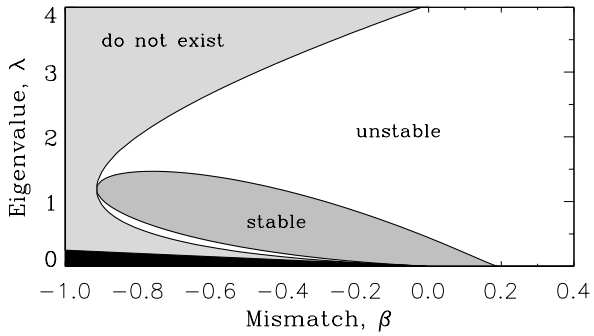

FIG. 7. Regions of existence and stability of solitons in the (λ,β)-plane. In the black region $\lambda \leq \lambda_{\rm cut}$ and no localized solutions exists. The V-solutions exist everywhere else, but are always unstable. η=2ρ=16, s=1.

We have made a series of calculations as shown in Fig. 6, found $dP/d\lambda$, and identified the regions of stability of the soliton solutions in the parameter plane (λ, β). The results are summarized in Fig. 7. We see that the quadratic nonlinearity allows stable bright solitons to exist for focusing Kerr nonlinearity, provided the effective mismatch parameter is sufficiently small, $-0.913 \leq \beta \leq 0.19$. This is in sharp contrast to purely

cubic bulk media, described by the 2D NLS equation, in which no stable solutions exist.

In Fig. 8 we show the regions of existence and stability of the soliton solutions in the parameter plane (P, β). Stable solutions are seen to require not only moderate values of the effective mismatch β, but also sufficiently low powers, $P \leq 3.2$.

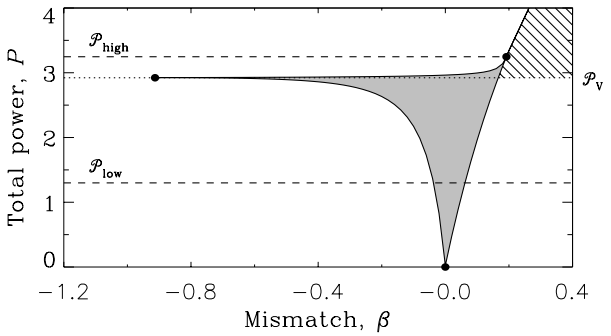

FIG. 8. Existence and stability regions of solitons as function of the total power P and mismatch β. Stable solitons exist in the shaded region, while unstable solutions exist in both the shaded and hatched regions. The unstable V-solutions exist on the dotted line. In the white region no localised solutions of the form (10) exist. The dashed lines indicate the values $\mathcal{P}_{\rm low}$=1.3 and $\mathcal{P}_{\rm high}$=3.2. η=2ρ=16, s=1.

It is interesting to compare the results in Fig. 8 with the analytical predictions that can be obtained from the so-called virial theory (see Appendix A), given by Eqs. (A3-A4). A rigorous result of virial theory is that no collapse can occur for powers below $\mathcal{P}_{\rm low}$=1.3. Our results show that unstable solutions do exist with powers below 1.3, but because they are based upon linear stability theory, they do not predict the nature of the instability. However, numerical simulation of Eqs. (1-2) have confirmed that the instability is indeed not a collapse instability for P<1.3.

Using virial theory one can estimate the threshold power for collapse to be $\mathcal{P}_{\rm high}$=3.2. This is strongly supported by our calculations, which shows that no stable solitons exist for P>3.2, corresponding exactly to $\mathcal{P}_{\rm high}$. However, again our results do not show the nature of the instability of the solitons with higher powers, and we have to perform numerical simulations. The results of these confirm that solitons with powers P>3.2 indeed collapse after a finite propagation distance.

V. COLLAPSE IN THE NLS LIMITS

Even though all solutions in the hatched region in Fig. 8 are (collapse) unstable, this region is nevertheless extremely interesting. In Fig. 9 we show the power versus β, as in Fig. 8, but focusing on the hatched region. The lower limit of the power in the solutions in this region is always that of the V-solution, $\mathcal{P}_V = P^c_{\rm nls}/4$, while the upper limit asymptotically approaches that of the W-solutions, $\mathcal{P}_W = P^c_{\rm nls}$, as β increases.

Thus, in the limit of large phase-mismatch, $\beta \gg 1$, the system (1-2) has collapse unstable solutions with powers in between the two NLS limits, $\mathcal{P}_V \leq P \leq \mathcal{P}_W$. In the lower NLS limit the fundamental is zero and the second harmonic is given by the 2D NLS equation (14). In the upper NLS limit, the second harmonic is approximately zero and the fundamental is given by the 2D NLS equation (12). In contrast, in the (one-field) 2D NLS equation itself, solutions only exist for one value of the power.

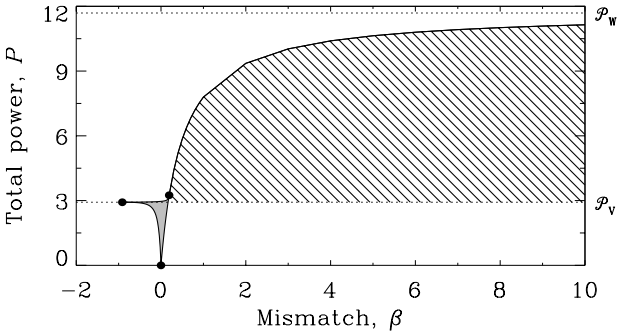

FIG. 9. Power P versus mismatch β as in Fig. 8 with the two dotted lines indicating the powers of the V- and W-solutions.

One might argue that the "true NLS limit" is the limit of large phase-mismatch, where the solution tends to the W-solution. The power of this solution is exactly the NLS power, $\mathcal{P}_W = P^c_{\rm nls}$, independently of the parameters η and ρ, in contrast to the power of the V-solutions in the other limit, which depends on η. Furthermore, the large phase-mismatch limit is also the one in which it has been proven that the cascaded $\chi^{(2)}$ nonlinearity has effective cubic properties (see [1]). However, from the point of view of the solutions to Eqs. (1-2), both limits have the characteristic NLS properties, and thus we stick to the notion of the two NLS-limits.

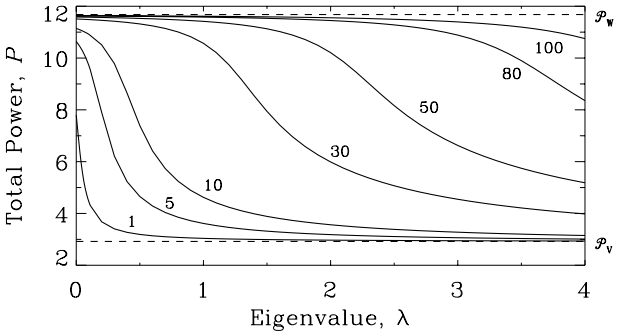

FIG. 10. Power versus λ for different values of β, indicated at the curves. The two dotted lines indicate the powers of the V- and W-solutions.

In Fig. 10 we have depicted P versus λ for several values of $\beta \geq 1$. Here we clearly see the properties discussed above. Regardless the value of β, the power will always asymptotically decrease toward $\mathcal{P}_V$, as the eigenvalue increases. At a given point λ_1 the solution will bifurcate into the V-solution with the exact power $\mathcal{P}_V$, as we know from Figs. 1 and 6. Correspondingly, regardless the value of λ, the power will always increase asymptotically to $\mathcal{P}_W$ as the mismatch β increases. However, there will never be a bifurcation of the solution into the W-solution. Finally, we see that the derivative $dP/d\lambda$ tends to zero as either of the NLS-limits is approached, in which case the solution is so-called marginally stable, as the solution to the 2D NLS equation [23].

Another interesting question regarding the two-component solutions in the hatched region, is which of the fields will be the one to initiate the collapse. Physical reasoning says it should be the one with the highest power. To confirm this we show in Fig. 11 the evolution of the (maximum) center amplitudes of the two fields, as obtained from numerical simulation of Eqs. (1-2) for λ=2, in the middle of the region in Fig. 10. We have not specifically perturbed the solutions, since the perturbations caused by the discretization in the numerical scheme, should be enough to make them collapse [24].

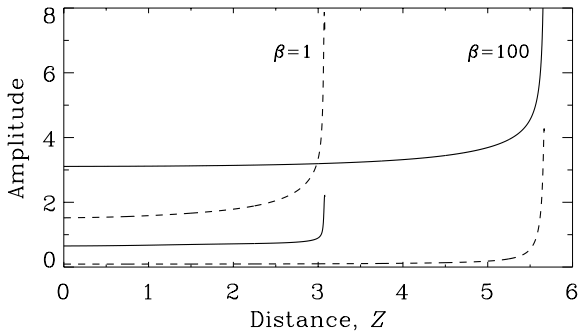

FIG. 11. Evolution of the center amplitudes of the fundamental (solid) and second-harmonic (dashed) waves for λ=2, and β=1,100, as obtained from numerical simulation of Eqs. (1-2). η=2ρ=16, s=1.

For β=1 the solution is close to the V-solution, and thus the second harmonic dominates over the fundamental. The specific contribution of the two fields to the total power is P_w=0.29 and $4P_v$=2.69. Correspondingly we see that it is the second harmonic that initiates the collapse. For β=100 the solution is close to the W-solution, and thus the fundamental instead dominates the second harmonic. The specific contribution of the two fields to the total power is now P_w=11.55 and $4P_v$=0.01. As expected it is now the fundamental that initiates the collapse. For β=1, the relative deviation of the power from the limit $\mathcal{P}_V$=3.25 is 8%. For β=100, the corresponding deviation of the power from the limit $\mathcal{P}_W$=11.69 is only 1%, Since the solutions are marginally stable in the NLS limits, the smaller deviation for β=100 could explain the longer collapse distance.

An important observation from Fig. 11 is that even though one of the fields is the dominant and initiates the collapse, the other field is always "dragged along" in the final stage of the collapse. This seems to be a general property, and was also observed in [6].

VI. DISCUSSION

We have analyzed the structure, and existence and stability properties of bright spatial solitary waves propagating in a lossles bulk $\chi^{(2)}$ medium under conditions for type I SHG, when focusing cubic (or Kerr) nonlinearity is taken into account. In bulk media with only focusing cubic nonlinearity, such beams are known to always be unstable, i.e. they either diffract or self-focus until a catastrophic collapse, depending on their incident power. In contrast, we have shown that a sufficiently strong quadratic nonlinearity can prevent the catastrophic self-focusing and enable such beams to exist and be stable in media with focusing cubic nonlinearity.

We have found that in order for stable bright spatial solitary waves (henceforth solitons) the effective phase-mismatch β must be sufficiently low, $-0.913 \leq \beta \leq 0.19$, otherwise they will always be unstable. In terms of physical variables (see Section II) this means that

$$-1.19 < \frac{|x_3|}{x_2^2/\kappa} = 1.3 \cdot \beta < 0.25 \qquad (16)$$

where $\kappa \equiv n_1^2 \Delta k/k_1$, with n_1 being the refractive index at the fundamental frequency, and $x_2 = \tilde{\chi}_1^{(2)}/[1\mathrm{pm/V}]$ and $x_3 = \tilde{\chi}_{1s}^{(3)}/[1\mathrm{pm}^2/\mathrm{V}^2]$ are the quadratic and cubic nonlinearities, respectively, measured in MKS units.

¿From the relation (16) we see that the cubic nonlinearity, whose strength is proportional to $\tilde{\chi}_{1s}^{(3)}$, must be sufficiently weaker than the quadratic nonlinearity, whose strength is proportional to $[\tilde{\chi}_1^{(2)}]^2/\Delta k$, in order for stable bright spatial solitary waves to exist.

Thus even a weak $\chi^{(2)}$-component can arrest self-focusing and enable stable solitons to exist, provided the fundamental and second harmonic waves are nearly phase matched. This effect is solely due to a competition between an effective phase-dependent self-defocusing of the quadratic nonlinearity, and the intensity-dependent self-focusing of the cubic nonlinearity. It is qualitatively similar to the existence of stable solitary waves in a bulk medium with self-focusing cubic and defocusing quintic nonlinearities.

We have shown that when stable brigth solitons exist, they always have a dimensionles powers P, which is below 3.2. This corresponds to the real physical power

$$P_0 P \leq 61\mathrm{kW} \cdot \left(\frac{10^3}{|x_3|}\right), \qquad (17)$$

for a fundamental wavelength of λ_1=1.3μm. Importantly, this power threshold for the existence of stable beams in bulk media with competing quadratic and cubic nonlinearities, is in good agreement with the prediction of the threshold power for collapse, which can be predicted analytically by the so-called virial theory [6], an effective tool for analyzing wave collapse.

VII. ACKNOWLEDGEMENTS

Part of this work has been supported by the Department of Industry, Science and Tourism, through grant no. 74 under the International S&T program.

APPENDIX A: VIRIAL THEORY

To obtain predictions about the dynamics we construct a so-called "virial" identity, in analogy with studies of collapse in the NLS equation [23] and the pure $\chi^{(2)}$ system [6]. This consists in the second derivative with respect to z of the virial $R^2(z)$ (for details see [6]):

$$\partial_z^2 R^2 = \frac{4}{P}[2(H-\beta P_v) + \mathrm{Re}\{\int w^2 v^* \, d\vec{r}\}], \qquad \text{(A1)}$$

where $R(z)$=$[P^{-1}\int r^2(|w|^2+4|v|^2)\,d\vec{r}\,]^{1/2}$ is the mean wave radius and r^2=x^2+y^2. ¿From Eq. (A1) we see that collapse of the solutions w and v, in the sense $R(z)\to 0$ at a finite z, will take place if the right hand side is negative definite. It was rigorously proven in [6], that if both individual norms are below a given threshold for all z,

$$P_w(z) < P_w^c = \frac{P_{\rm nls}^c}{1+\rho},\ P_v(z) < P_v^c = \frac{P_{\rm nls}^c}{\lambda+\rho}, \qquad \text{(A2)}$$

then such a collapse can never occur. To assure that Eq. (A2) is satisfied for all z the total norm must be sufficiently low,

$$P < \mathcal{P}_{\rm low} = \min\{P_w^c, 4P_v^c\}. \qquad \text{(A3)}$$

Furthermore, we can estimate that collapse should possibly occur if the total norm is sufficiently high,

$$P > \mathcal{P}_{\rm high} \equiv P_w^c + 4P_v^c, \qquad \text{(A4)}$$

under the additional requirement H<0. We stress that the limit (A3) is a rigorous result, while (A4) is only an estimate based on a comparison with pure $\chi^{(3)}$ media [6]. In the intermediate range $\mathcal{P}_{\rm low}$<P<$\mathcal{P}_{\rm high}$ nothing definite can be concluded the virial identity.

These predictions were tested numerically for β=0 and positive values of λ and ρ, which verified the lower bound (A3), and showed that the upper bound (A4) was reliable, except for a narrow region of the parameter space, where it was slightly underestimated [6,12]. In the particular case η=2ρ=16, it was shown numerically in [12], that $\mathcal{P}_{\rm high}$ is a reasonable estimate of the actual threshold power for moderate values of β, i.e. $|\beta|\leq$4.

[1] G.I. Stegeman, D.J. Hagan, and L. Torner, J. Opt. Quantum Electron. **28**, 1691 (1996).

[2] K. Hayata and M. Koshiba, Phys. Rev. Lett. **71**, 3275 (1993). V.V. Steblina, Yu.S. Kivshar, M. Lisak, and B.A. Malomed, Opt. Comm. **118**, 345 (1995). A.V. Buryak, Yu.S. Kivshar, and V.V. Steblina, Phys. Rev. A **52**, 1670 (1995). L. Torner, D. Mihalache, D. Mazilu, E.M. Wright, W. Torruellas, and G.I. Stegeman, Opt. Comm. **121**, 149 (1995).

[3] W.E. Torruellas, Z. Wang, D.E. Hagan, E.W. Van Stryland, G.I. Stegeman, L. Torner, and C.R. Menyuk, Phys. Rev. Lett. **74**, 5036 (1995). R.A. Furst, B.L. Lawrence, W.E. Torruellas, and G.I. Stegeman, Opt. Lett. **22**, 19 (1997).

[4] L. Torner, C.R. Menyuk, W.E. Torruellas, and G.I. Stegeman, Opt. Lett. **20**, 13 (1995).

[5] L. Torner and E.M. Wright, J. Opt. Soc. Am. B **13**, 864 (1996). G. Leo, G. Assanto, and W. Torruellas, J. Opt. Soc. Am. B **14**, 3134 (1997).

[6] L. Bergé, O. Bang, J.J. Rasmussen, and V.K. Mezentsev, Phys. Rev. E **55**, 3555 (1997).

[7] A. Kobyakov, F. Lederer, O. Bang, and Yu.S. Kivshar, Opt. Lett. (in press).

[8] A.V. Buryak, Y.S. Kivshar, and S. Trillo, Opt. Lett. **20**, 1961 (1995). S. Trillo, A.V. Buryak, and Y.S. Kivshar, Opt. Comm. **122**, 200 (1996).

[9] M.A. Karpierz, Opt. Lett. **20**, 1677 (1995).

[10] O. Bang, J. Opt. Soc. Am. B **14**, 51 (1997).

[11] O. Bang, Yu.S. Kivshar, A.V. Buryak, Opt. Lett. **22**, 1680 (1997).

[12] O. Bang, L. Bergé, and J.J. Rasmussen, Opt. Comm. (in press).

[13] A. De Rossi, G. Assanto, S. Trillo, and W. Torruellas, Opt. Comm. (accepted).

[14] C.B. Clausen, O. Bang, and Yu.S. Kivshar, Phys. Rev. Lett. **78**, 4749 (1997).

[15] M.G. Vakhitov, A.A. Kolokolov, Radiophys. Quantum Electron. **16**, 783 (1975).

[16] N.E. Kosmatov, V.F. Shvets, and V.E. Zakharov, Physica D **52**, 16 (1991).

[17] D. Anderson, M. Bonnedal, and M. Lisak, Phys. Fluids **22**, 1838 (1979).

[18] M. Grillakis, J. Shatah, and W. Strauss, J. of Func. Anal. **74**, 160 (1987).

[19] D.E. Pelinovsky, A.V. Buryak, and Yu.S. Kivshar, Phys. Rev. Lett. **75**, 591 (1995).

[20] A.V. Buryak, Yu.S. Kivshar, and S. Trillo, Phys. Rev. Lett. **77**, 5210 (1996).

[21] Y. Chen, Phys. Lett. A **234**, 443 (1997).

[22] D.E. Pelinovsky, V.V. Afanasjev, and Yu.S. Kivshar, Phys. Rev. E **53**, 1940 (1996).

[23] J.J. Rasmussen and K. Rypdal, Physica Scripta **33**, 481 (1986).

[24] O. Bang, J.J. Rasmussen, and P.L. Christiansen, Nonlinearity **7**, 205 (1994).